ChemComm

Accepted Manuscript

This article can be cited before page numbers have been issued, to do this please use: A. K. Das, A. Biswas, S. Malferrari and D. M. Kalaskar, *Chem. Commun.*, 2018, DOI: 10.1039/C7CC09051J.

This is an Accepted Manuscript, which has been through the Royal Society of Chemistry peer review process and has been accepted for publication.

Accepted Manuscripts are published online shortly after acceptance, before technical editing, formatting and proof reading. Using this free service, authors can make their results available to the community, in citable form, before we publish the edited article. We will replace this Accepted Manuscript with the edited and formatted Advance Article as soon as it is available.

You can find more information about Accepted Manuscripts in the author guidelines.

Please note that technical editing may introduce minor changes to the text and/or graphics, which may alter content. The journal's standard Terms & Conditions and the ethical guidelines, outlined in our author and reviewer resource centre, still apply. In no event shall the Royal Society of Chemistry be held responsible for any errors or omissions in this Accepted Manuscript or any consequences arising from the use of any information it contains.

View Article Online
DOI: 10.1039/C7CC09051J

Authors

Ankan Biswas,[a] Sara Malferrari,[b] Deepak M. Kalaskar[b] and Apurba K. Das*[a]

Affiliations

[a] Department of Chemistry, Indian Institute of Technology Indore, Khandwa Road, Indore 453552, India. E-mail: apurba.das@iiti.ac.in

[b] Institute of Orthopaedics & Musculoskeletal Science, Division of Surgery and Intervention Science, Royal National Orthopaedic Hospital, University College London, Brockely Hill, Stanmore, Middlesex HA7 4LP, UK

Acknowledgements

A.K.D. sincerely acknowledges NanoMission, Department of Science & Technology (Project: SR/NM/NS-1458/2014), New Delhi, India for financial support. A.B. sincerely acknowledges MHRD, Government of India for his doctoral fellowship. Authors thank SAIF, IIT Bombay for TEM facility and SIC, IIT Indore for providing required instrumental facilities. D.M.K. would like to thank UCL Global Engagement Fund for supporting collaborative work.

View Article Online
DOI: 10.1039/C7CC09051J

Journal Name

COMMUNICATION

Arylboronate esters mediated self-healable and biocompatible dynamic G-quadruplex hydrogels as promising 3D-bioink

Received 00th January 20xx,
Accepted 00th January 20xx

DOI: 10.1039/x0xx00000x

www.rsc.org/

Extrudable G-quadruplex hydrogels were prepared at physiological pH. Gels with suitable mechanical properties were explored as 3D-bioink. The 3D printing process is driven by injectability, highly thixotropic and self-healable nature of the gel. High cell viability and homogeneous cell distribution within the gel make it a promising material as 3D bio-ink.

Molecular self-assembly is exploited as one of the effective strategies to make hydrogels.[1] Hydrogels have been used in various applications including cell culture, drug delivery, separation of biomolecules, tissue engineering and 3D printing.[2] 3D printing is a rapidly growing technology having capability to generate 3D objects through deposition of multiple layers of printable materials. During 3D printing, biomaterials including cells, drugs and growth factors can be mixed with printable materials (bioink) for useful biomedical applications like drug testing, in vitro 3D disease model, tissues and organ printing.[3] The principal requirements of the use of hydrogels as bioink are that the hydrogels should be: i) biocompatible, ii) printable (continuous and homogenous material extrusion, devoid of air bubbles, having printing pressure compatible with cell viability: thus shear-thinning gels are preferred), iii) possess enough mechanical strength to support cells, achieve high resolution and hold the 3D structure (generally G' close to 1 kPa), iv) suitable structure stability (immediate structure stability during printing), and v) fast post-printing crosslinking kinetics, compatible with cell viability.[4] Majority of reported hydrogels are based on natural or synthetic polymers.[4,5] However their use as bioink is limited due to lack of printability and biocompatablity. Self-healing physical polymeric hydrogels possess low mechanical strength and stability.[6] Chemically crosslinked polymers often create trapped airbubbles, slow crosslinking post-prinitng, and inhomogeneity in printed structures.[4,6] Only handful of bioink are available based on natural polymers, which suffer from their clinical use due to compositional variabilities. Synthetic polymeric hydrogels are also limited in number and thus their use is also limited for targeted applications.[4] Low molecular weight (LMW) dynamic self-healing extrudable hydrogels can be used as bioink due to their i) biodegradable nature, ii) reversibility, iii) better homogeneity, and iv) tunable properties.[7] However, to date, use of self-healing LMW based hydrogels as 3D bioink is infancy. Current work explores the use of suitable LMW based self-healing hydrogels as bioink.

Boronic acids are well known to form dynamic covalent cyclic boronate esters with *cis*-1,2-diols.[8] Dynamic covalent character of the molecules generates unique self-healing and injectable properties within the hydrogels.[9] Guanosine contains cis-1,2-diol which can form dynamic boronate esters and also guanosine analogs are known to form G4-quartet. G4 hydrogels are stabilized by metal ions, especially with K^+ ion.[10] Columnar stacking of G4-quartet by π-π stacking interaction gives higher aggregate G-quadruplex structure.[11] There are several drawbacks of G4 hydrogels such as i) the materials have tendency to precipitate out from the gel state, ii) poor solubility of guanosine and iii) the requirement of large amount of metal ions.[12] Davis *et al* have reported G4 hydrogels by potassium borate and guanosine and studied the role of anion, cation and aromatic dyes on their stability.[13] They have also demonstrated self-destructive nature of 5'-iodoguanosine hydrogel and controlled release of acyclovir drug from the gel.[14] Recently, Shi *et al* have applied imine based G4 hydrogel for efficient drug release.[15] Sadler *et al* reported photoactivable G4 hydrogel for anticancer drug delivery.[16] These recent reports on G4 borate hydrogels show potential applications in several biological aspects. Several poly-boronic acids with multifunctional diols or poly-diols with diols with multifunctional boronic acids based hydrogels have also been reported in the literature.[17]

[a] *Address here.*
[b] *Address here.*
† Footnotes relating to the title and/or authors should appear here.
Electronic Supplementary Information (ESI) available: [details of any supplementary information available should be included here]. See DOI: 10.1039/x0xx00000x

View Article Online
DOI: 10.1039/C7CC09051J

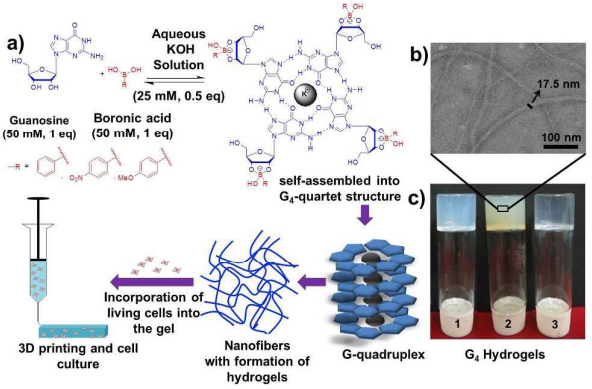

Fig. 1 (a) Schematic representation of G4-quadruplex self-assembly process and 3D printing, cell culture applications. (b) TEM image of 4-GNPBA hydrogel. (c) Optical images of hydrogels: GPBA (vial 1), 4-GNPBA (vial 2) and 4-GMPBA (vial 3).

Herein, three hydrogels were made up with phenyl boronic acid (PBA), 4-nitrophenyl boronic acid (4-NPBA) and 4methoxyphenyl boronic acid (4-MPBA) with guanosine (G). Hydrogels were prepared by heating (80 °C) of the suspension of poorly soluble guanosine in aqueous KOH solution with PBA, 4-NPBA and 4-GMPBA. The molar ratio (concentration) of G, boronic acids and KOH were 1:1:0.5 (50 mM, 50 mM and 25 mM) (Fig. 1). Gels from G with PBA (GPBA) and 4-NPBA (4-GNPBA) were strong and promising for 3D printing applications. However, G and 4-MPBA (4-GMPBA) formed a weak gel. Final pHs of the gels were observed as 7.6. Gel was not formed in acidic conditions (pH < 7) due to unstable nature of boronate esters and absence of reactive anionic borates (Fig. S1).[9b,18] Basic conditions are favourable for boronate ester formation.[18] At higher pH (pH > 9), guanosine losses –N1-H proton and thus weak gel was formed due to loss of intermolecular H-bonding.[19] So, both acidic and higher pHs are not suitable for 3D printing. Gel at pH ~ 7.6 was suitable for biological assay and 3D printing. GPBA and 4-GNPBA are stable over a period of 8 months and 3 months respectively. However, 4-GMPBA crystallized after a week. TEM images of hydrogels display entangled nanofibrils (Fig. 2, Fig. S2). The average diameters of the fibrils are 15-20 nm with several micrometres in length. TEM images suggest that various G4-quartets self-assembled with each other to form aggregated nano-fibrils. All the gels are thermo-reversible in nature (Fig. S1). At a molar ratio of 1:1:1 (G: boronic acid: KOH; 50 mM each), weak gels were formed (Fig. S1). NaOH, LiOH and KCl were also used to form GPBA (Fig. S1). However, the satisfactory results were not obtained. In presence of NaOH, weak gel was formed. LiOH produced free flowing transparent liquid. At higher concentration of KCl (100 mM), gel was formed but precipitation occurred within 2 hours (Fig. S1). These results suggest that suitable conditions are very crucial for the gelation. Formation of boronate esters during gelation was confirmed by ^{11}B NMR (Fig. S3). After formation of boronate ester, peak shifts to the higher field in ^{11}B NMR.[15,18] In GPBA gel, peak attributed by respective boronate ester was observed at 10.93 ppm with free PBA (29.95 ppm). Peaks at 8.14 ppm and 8.34 ppm are observed for boronate esters of 4-GNPBA and 4-GMPBA respectively. In 4-GNPBA, 4-NPBA is almost completely converted into boronate ester. Negative resonance (–R) effect of strong electron withdrawing *p*-NO2 group in 4-NPBA makes the boron centre more electrophilic i.e. more reactive towards nucleophiles (diols). Contrary to 4-GNPBA, the conversion of 4-GMPBA is lowest among three hydrogels due to the presence of electron donating *p*-OMe group of 4-MPBA. Temperature dependent ^{11}B NMR experiment was performed with GPBA (Fig. S4). Thermal effect on ester formation is observed. With increase in temperature from 25 °C to 50 °C; intensity of ester peak is increased. ^{11}B NMR spectra at different pHs show that the equilibrium is highly dependent on pH (Fig. S5, Table S1). At higher pH, boronate ester formation is favourable and free boronic acid peak shifts towards upfield due to the presence of anionic tetrahedral borates as major species.[18] Ester was not formed at acidic pH.[9b,18]

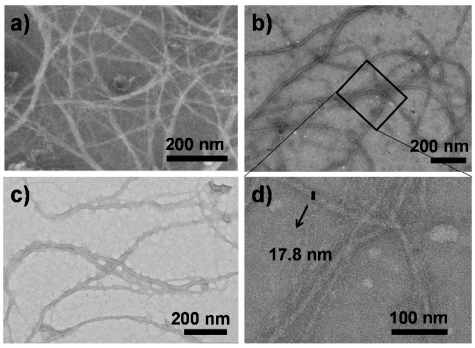

Fig. 2 TEM images of a) **GPBA**, b) **4-GNPBA** and c) **4-GMPBA** hydrogels showing nano-fibrillar morphology. d) Magnified TEM image of **4-GNPBA**

Circular Dichroism (CD) is an effective tool to determine the supramolecuar secondary structure of the self-assembled molecules. In CD spectrum of GPBA hydrogel, two positive peaks at 290 nm and 240 nm with a negative peak at 260 nm are observed (Fig. 3). The opposite CD signatures at 290 nm and 260 nm are characteristic peaks for head to head stacked G4-quartets and opposite sign bands at 240 nm and 260 nm are attributed for head to tail stacked G4-quatrets.[13a] Overall CD signature suggests that GPBA hydrogel exhibits with mixture of head to head and head to tail G4-quartets. An additional sharp peak is appeared at 231 nm, which is attributed due to aromatic ring of PBA. 4-GNPBA shows two positive peaks at 250 nm and 284 nm (Fig. 3), that is attributed by stacking of several G4-quartets.[13b] Two positive peaks at 290 nm and 240 nm along with a negative peak at 257 nm are observed in 4-GMPBA which is similar with GPBA (Fig. 3). Also an additional peak appears at 221 nm for aromatic ring of 4-MPBA.

Powder X-ray diffraction (PXRD) studies of all the three gels show 2θ value associated with d ≈ 3.3 Å, which is attributed by the π-π stacking distance between G4-quatrets (Fig. S6).[13b]

View Article Online
DOI: 10.1039/C7CC09051J

Additional peaks at d = 3.58 Å in case of GPBA and d = 3.82 Å in case of 4-GNPBA are attributed by the π-π stacking interaction between aromatic phenyl rings of the respective boronate esters (Fig. S6a, S6b). Such additional interaction is not observed in in 4-GMPBA (Fig. S6c). These results suggest that

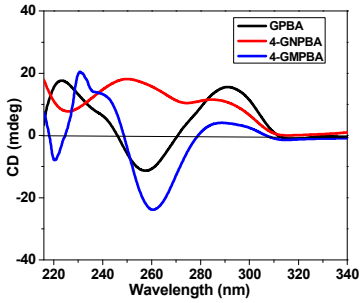

Fig. 3 CD spectra of **GPBA**, **4-GNPBA** and **4-GMPBA** showing formation of G-quadruplex.

several G4-quratets self-assemble with each other through π-π stacking to build G-quadruplex supramolecular structure and stabilizes the gels. However, other amorphous gels stabilized by non-covalent interactions or chemical crosslinking can be used as 3D bio-ink if they achieve suitable mechanical and biocompatible properties.

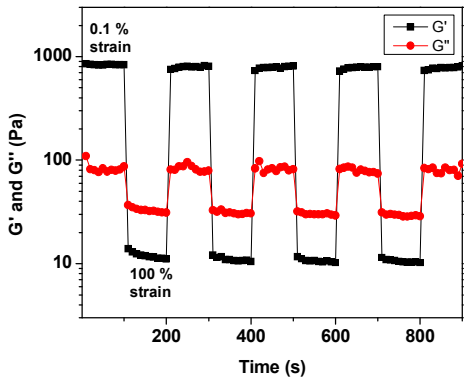

Fig. 4 Thixotropic property of **GPBA** gel. The gel show quick recovery of gel state (G´ > G´´) from sol state (G´´>G´) under cyclic dynamic strain sweep experiment.

After characterization of hydrogels, mechanical properties of the gels were studied by rheology. The frequency sweep experiment of the gels was carried out within angular frequency range 100–0.05 rad s^{-1} at a constant strain of 0.1%. Throughout the experiment, the elastic storage modulus (G´) was consistently greater than the loss modulus (G´´) for all three gels, which demonstrates the viscoelastic property of the gels over the whole angular frequency range (Fig. S7). Frequency sweep study showed that G´ values of the gels followed the order: GPBA (850 Pa)> 4-GNPBA (300 Pa)> 4-GMPBA (100 Pa) at angular frequency of 10 rad s^{-1}. Lower G´ value, descending pattern of both G´ and G´´ and less gap between G´ and G´´ of 4-GMPBA describe liquid-like nature of the gel. Initially, G´ value was comparatively higher (650 Pa at angular frequency of 100 rad s^{-1}) for 4-GNPBA but it was decreased with decrease in angular frequency up to 10 rad s^{-1} and then it was steady throughout the experiment up to 0.05 rad s^{-1}. G´ value of GPBA gel was almost constant for the whole experiment process which reveals strong and stable nature of the gel. Rheological data are in well agreement with the TEM images, where the fibril densities decrease from GPBA to 4-GNPBA to 4-GMPBA hydrogels. Cyclic dynamic strain sweep experiment was performed to investigate thixotropic and self-healing properties of GPBA (Fig. 4). In this experiment, alternative 0.1% (lower) and 100% (higher) strain (at a constant angular frequency 10 rad s^{-1}) were applied on the gel over a period of 900 seconds and successive 4 cycles. At higher

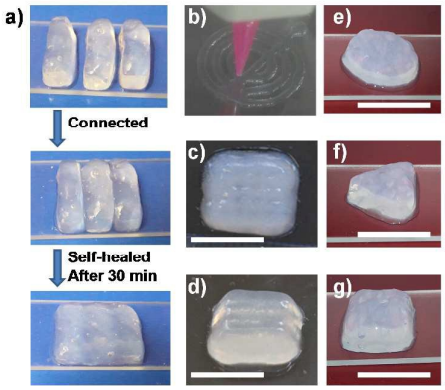

Fig. 5 (a) Visual observation of self-healing property of **GPBA** hydrogel. Three pieces of gels are self-healed to an integral piece after 30 min. (b) Injection of **GPBA** through 3D printing inkjet. (c) & (d) 3D printed block with **GPBA**. (Scale: 10 mm), (e)-(g) Different 3D geometrical patterns drawn by **GPBA** (scale = 10 mm).

strain (100%), viscoelastic property of the gel was lost (sol state, G´´>G´). However, in every successive step, it was self-healed quickly after coming back to lower strain (0.1%) with almost full recovery of initial viscoelastic nature. After mechanical study, three pieces of GPBA gel were connected with each other for visual observation of self-healing property (Fig. 5a). After 30 minutes, the connection joint of gel pieces were well healed to give one integral piece without any external stimuli. Both rheological and visual observation of self-healing test suggests that GPBA gel is highly thixotropic and self-healable. Self-healing property of the hydrogel is anticipated to facilitate 3D printing process as printing layers can merge and heal together based on the dynamic nature of the gel. GPBA Hydrogels due to its unique thixotropic and self-healing behaviour found to maintain complex shape post 3D printing. GPBA was used as ink to print a 3D block with 20 layers (10 mm length and 5 mm height, height of each layer 0.25 mm) (Fig. 5c, 5d, Fig. S8) and other geometrical patterns (Fig. 5e-g).

To evaluate the biocompatibility of GPBA gel, cell viability test was performed using adult human dermal fibroblast (HDFs) cells for 24 h cell culture.[20] Fluorescence microscopic images of live/dead cell assay show 98% HDFs cells were viable in GPBA (Fig. 6a, Fig. S9), which was similar to nonprinted 3D hydrogel (control). Z-stack of fluorescence microscopic image of cells after encapsulation inside the GPBA gel displays stable homogeneous distribution of cells within the gel (Fig. 6b). Cell culture study shows that cells are viable after 3D printing process and can survive mechanical stress and pressure exerted on cells wall during printing process.

View Article Online
DOI: 10.1039/C7CC09051J

In conclusion, we have demonstrated synthesis of guanosine-arylboronate esters mediated dynamic G-quadruplex hydrogels in presence of K^+ ions. G-quadruplex assembly of guanosine purine moiety generates essential nanofibrillar networks for the encapsulation of water molecules to produce hydrogels. Dynamic nature of boronic acid-boronate ester equilibrium produces essential injectable, self-healing and thixotropic property for 3D printing. The gel is non-toxic and the printing process does not damage cell viability. This gel is ready to use and doesn't require additional crosslinking steps post-printing. Guanosine and PBA are relatively low-cost and readily available materials. Research on novel bio-ink for 3D printing is vital for progress of this technology for medical applications. This work thus paves way for use of low molecular weight biocompatible hydrogels for 3D bio-printing.

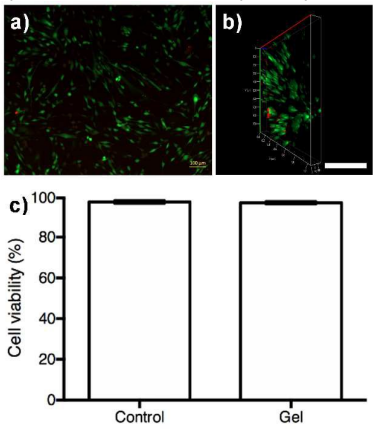

Fig. 6 a) Fluorescence microscopy images for live/dead cell assay of HDFs cell in **GBPA** hydrogel after 24 h cell culture (scale bar = 100 µm). b) Z-stack fluorescence microscopic 3D image shows adhered HDFs cells inside the 3D printed gel (scale bar = 500 µm). c) Cell viability graph shows 98% (w.r.t. control experiment) viability in **GPBA** hydrogel after 24 h incubation.

Conflicts of Interest

There are no conflicts to declare.

Notes and References

1 X. Du, J. Zhou, J. Shi and B. Xu, *Chem. Rev*., 2015, **115** , 13165.

2 (a) H. Y. Yoshikawa, F. F. Rossetti, S. Kaufmann, T. Kaindl, J. Madsen, U. Engel, A. L. Lewis, S. P. Armes and M. Tanaka, *J. Am. Chem. Soc*., 2011, **133**, 1367; (b) E. Secret, S. J. Kelly, K. E. Crannell and J. S. Andrew, *ACS Appl. Mater. Interfaces*, 2014, **6**, 10313; (c) J. J. Simhadri, H. A. Stretz, M. Oyanader and P. E. Arce, *Ind. Eng. Chem. Res*., 2010, **49**, 11867; (d) H. Tan, C. R. Chu, K. A. Payne and K. G. Marra, *Biomater.*, 2009, **30**, 2499; (e) F. Yang, V. Tadepalli and B. J. Wiley, *ACS Biomater. Sci. Eng*., 2017, **3**, 863.

3 (a) S. V. Murphy and A. Atala, *Nature Biotech.*, 2014, **32**, 773; (b) E. Vorndran, U. Klammert, A. Ewald, J. E. Barralet, and U. Gbureck, *Adv. Funct. Mater.*, 2010**, 20**, 1585; (c). E. D. Miller, J. A. Phillippi, J. W. Fisher, P. G. Campbell, L. M. Walker and L. E. Weiss, *Comb. Chem. High Throughput Screen*., 2009, **12**, 604.

4 A. Popov, S. Malferrari and D. M. Kalaskar, *J. 3D Print. Med*., 2017, **1**, 191.

5 (a) L. Ouyang, C. B. Highley, C. B. Rodell, W. Sun and J. A. Burdick, *ACS Biomater. Sci. Eng*., 2016, **2**, 1743. (b) L. R. Hart, S. Li, C. Sturgess, R. Wildman, J. R. Jones and Wayne Hayes, *ACS Appl. Mater. Interfaces*, 2016, **8**, 3115. (c) L. Shi, H. Carstensen, K. Hölzl, M. Lunzer, H. Li, J. Hilborn, A. Ovsianikov and D. A. Ossipov, *Chem. Mater*., 2017, **29**, 5816.

6 T. Jungst, W. Smolan, K. Schacht, T. Scheibel and J. Groll, *Chem. Rev*., 2016, **116**, 1496.

7 B. Vivek, P. Kumar and E. Prasad, *J. Phys. Chem. B*, 2016, **120**, 5262.

8 (a) W. L. A. Brooks and B. S. Sumerlin, *Chem. Rev*., 2016, **116**, 1375; (b) A. P. Bapat, D. Roy, J. G. Ray, D. A. Savin and B. S. Sumerlin, *J. Am. Chem. Soc*., 2011, **133**, 19832.

9 (a) H. Meng, P. Xiao, J. Gu, X. Wen, J. Xu, C. Zhao and J. Zhangand and T. Chen, *Chem. Commun*., 2014, **50**, 12277; (b) A. Pettignano, S. Grijalvo, M. Haring, R. Eritja, N. F. Tanchoux and D. Diaz Diaz. *Chem. Commun*., 2017, **53**, 3350.

10 (a) I. Bang, *Biochem. Z*., 1910, **26**, 293; (b) M. Gellert, M. N. Lipsett, D.R. Davies, *Proc. Natl. Acad. Sci. U.S.A*., 1962, **48**, 2013; (c) J. T. Davis, *Angew. Chem. Int. Ed*., 2004, **43**, 669.

11 (a) D. González-Rodríguez, J. L. J. van Dongen, M. Lutz, A. L. Spek, A. P. H. J. Schenning and E. W. Meijer, *Nat. Chem*., 2009, **1**, 151; (b) X. Shi, K. M. Mullaugh, J. C. Fettinger, Y. Jiang, S. A. Hofstadler and J. T. Davis *J. Am. Chem. Soc.*, 2003, **125**, 10830.

12 (a) B. Buchs, W. Fieber, F. Vigouroux-Elie, N. Sreenivasachary, J. M. Lehn and A. Herrmann, *Org. Biomol. Chem*., 2011, **9**, 2906; (b) B. Adhikari, A. Shah and H. B. Kraatz, *J. Mater. Chem. B*, 2014, **2**, 4802.

13 (a) G. M. Peters, L. P. Skala, T. N. Plank, B. J. Hyman, G. N. M. Reddy, A. Marsh, S. P. Brown and J. T. Davis, *J. Am. Chem. Soc*., 2014, **136**, 12596; (b) G. M. Peters, L. P. Skala, and J. T. Davis, *J. Am. Chem. Soc*., 2016, **138**, 134.

14 T. N. Plank and J. T. Davis, *Chem. Commun*., 2016, **52**, 5037.

15 Y. Li, Y. Liu, R. Ma, Y. Xu, Y. Zhang, B. Li, Y. An and L. Shi, *ACS Appl. Mater. Interfaces*, 2017, **9**, 13056.

16 V. Venkatesh, N. K. Mishra, I. R. Canelón, R. R. Vernooij, H. Shi, J. P. C. Coverdale, A. Habtemariam, S. Verma and P. J. Sadler, *J. Am. Chem. Soc.,* 2017, **139**, 5656.

17 (a) V. Heleg-Shabtai, R. Aizen, R. Orbach, M. A. Aleman-Garcia and I. Willner, *Langmuir*, 2015, **31**, 2237; (b) L. He, D. Szopinski, Y. Wu and G. A. Luinstra, *ACS Macro Lett*., 2015, **4**, 673; (c) S. Kitano, Y. Koyama, K. Kataoka, T. Okano and Y. A. Sakurai, *J. Controlled Release*, 1992, **19**, 161.

18 M. Bishop, N. Shahid, J. Yang and A. R. Barron, *Dalton Trans*, 2004, 2621.

19 V. Verdolino, R. Cammi, B. H. Munk and H. B. Schlegel, *J. Phys. Chem. B*, 2008, **112**, 16860.

20 A. Bruinik and R. Luginbuehl, in *Tissue Engineering III: Cell - Surface Interactions for Tissue Culture*, ed. C. Kasper, F. Witte and R. Pörtner, Springer, Berlin, 1st edn, 2012, vol. 126, ch. 5, pp. 117-152.